

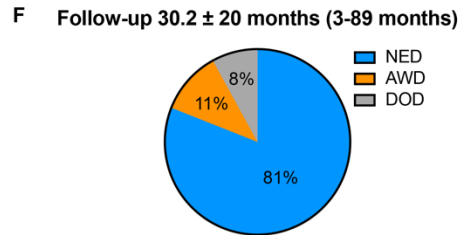
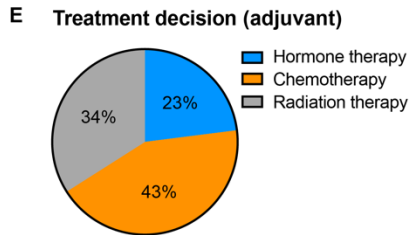
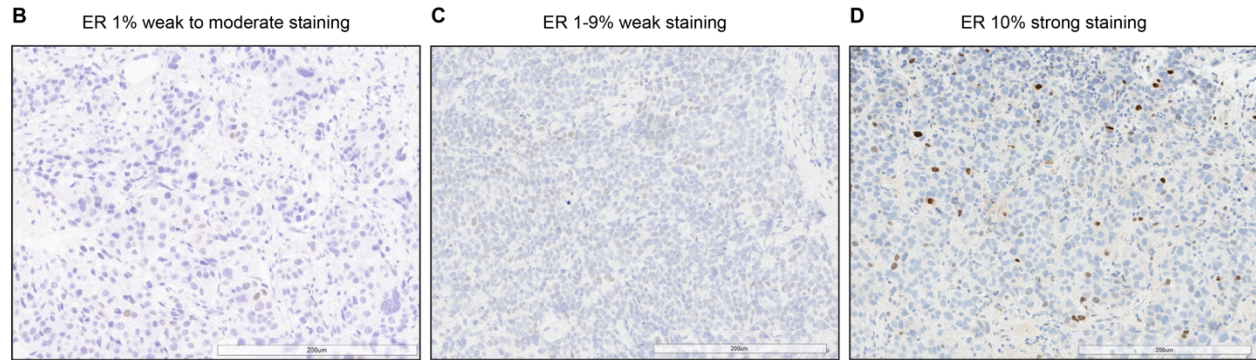
**Supplementary figures:**

**A**

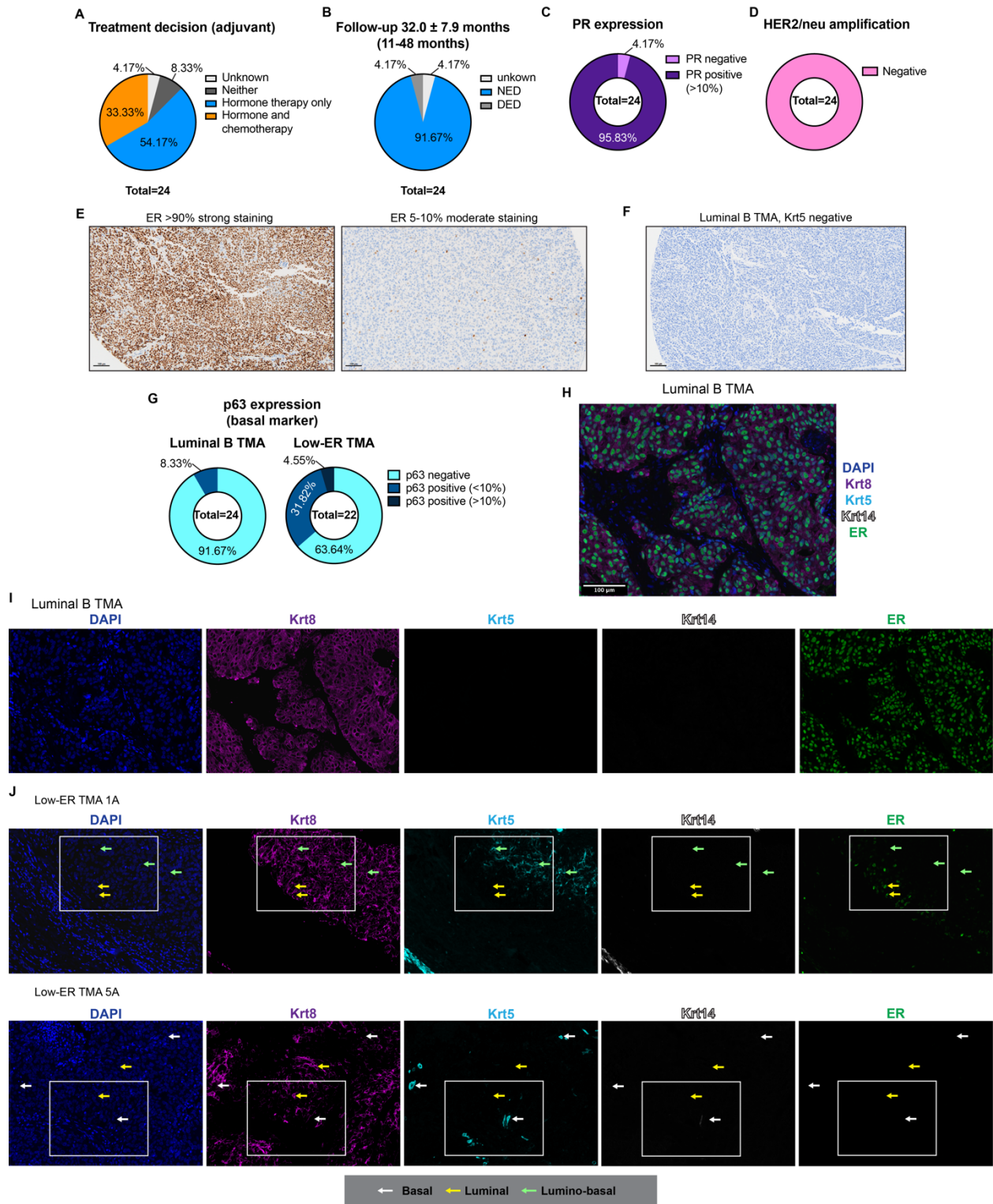
Histological features of 46 Low-ER positive carcinomas

Type	Invasive ductal carcinoma: 96% (44) Invasive lobular carcinoma: 4% (2)
Grade	High: 89% (41) Intermediate: 11% (5)
Size	2.97 ± 2.6 cm (range: 0.1 – 10.0 cm)
Ductal carcinoma in-situ present	55%
Lymphovascular invasion present	39%
Lymph node status	N0 = 30 (ITCs in two patients) N1 = 2    N2 = 0    N3 = 4
Response to neoadjuvant chemotherapy	Pathologic complete response = 75% (9/12) Pathologic partial response = 25% (3/12)* *Two had microinvasion only

Oncotype Recurrence Score (n=10) = 48.8 ± 12 (18-61)

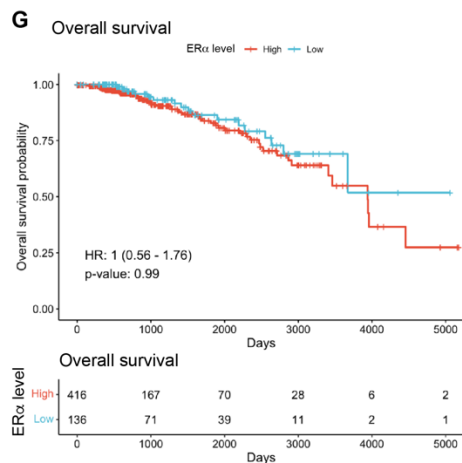
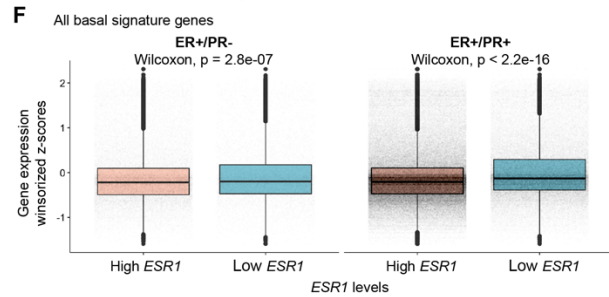
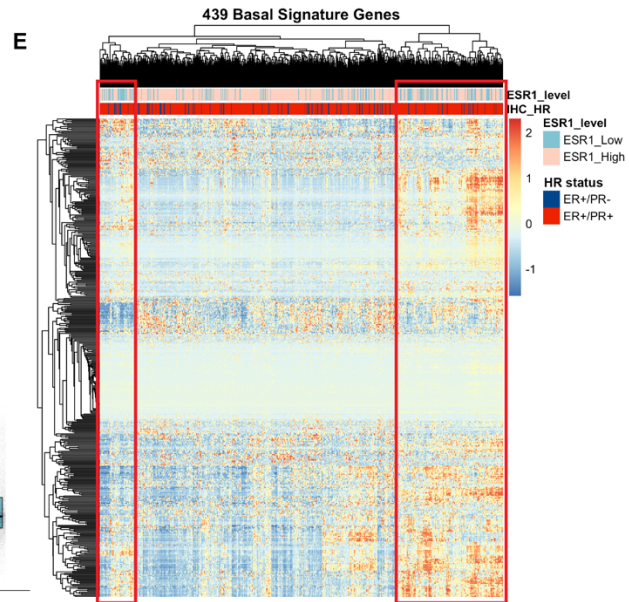
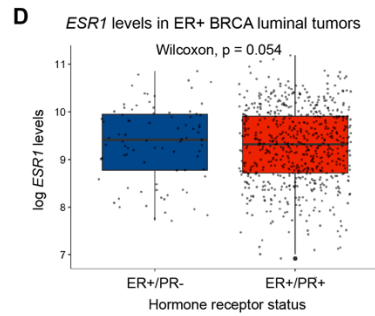
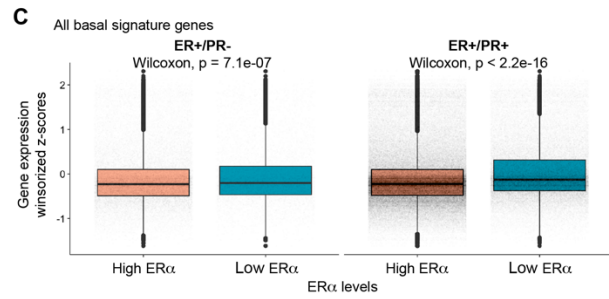
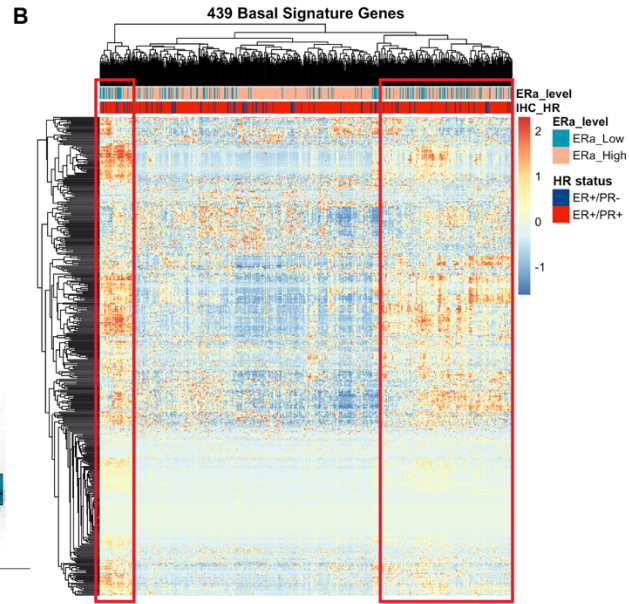
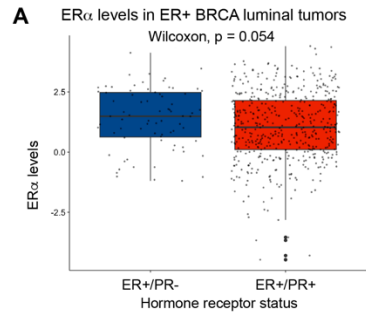


**Supplementary Figure 1: (A)** Histological features of the 46 low-ER cases in our cohort. **(B-D)** Representative IHC images showing the different levels and intensity of ER staining in the low-ER tumors. **(E-F)** Breakdown of treatment decisions **(E)**, and follow-up details **(F)**, of the 46 low-ER cases.

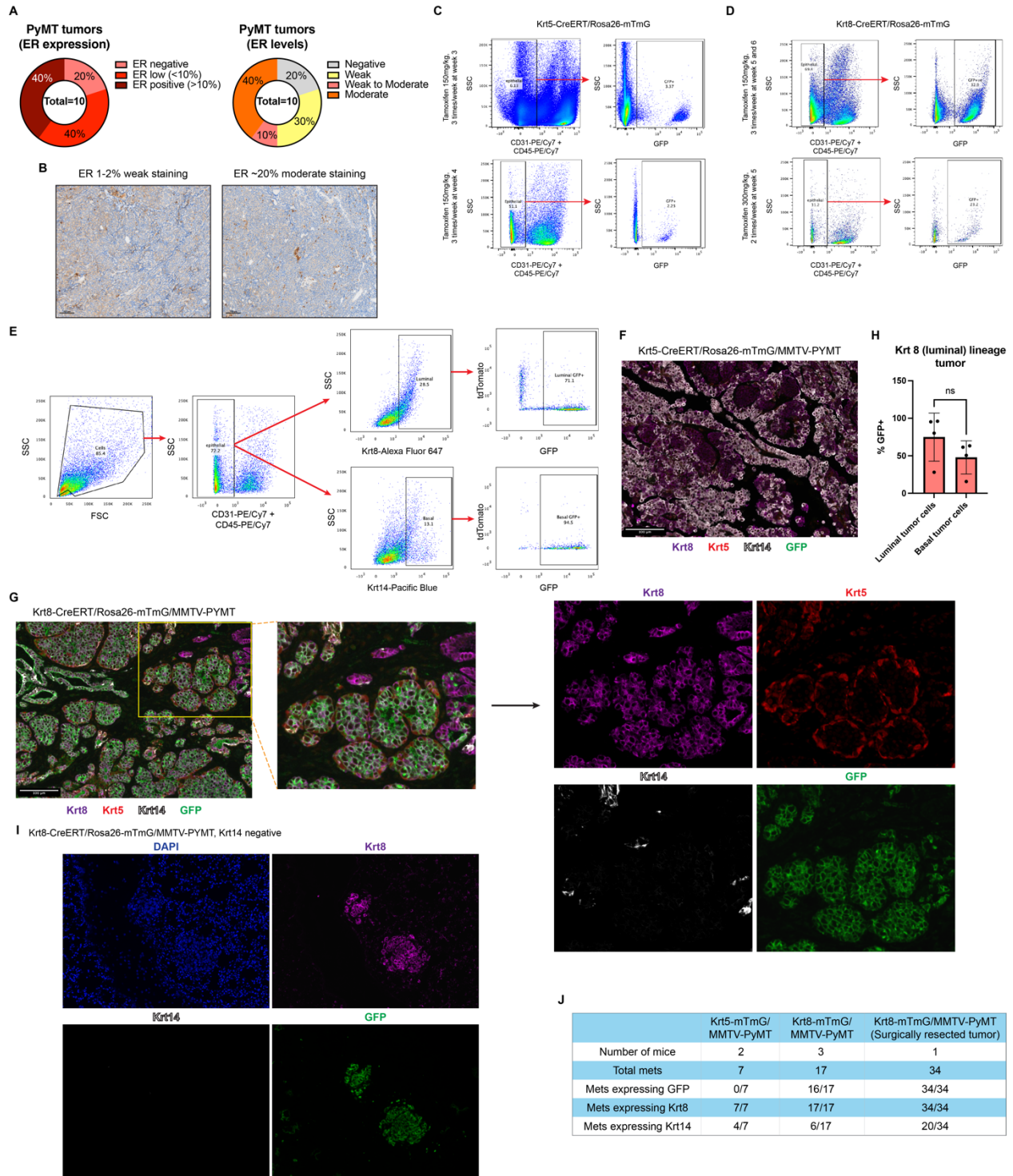


**Supplementary figure 2: (A-D) Breakdown of treatment decisions (A), follow-up details (B), PR expression (C), and Her2/neu amplification (D), of the 24 luminal B cases used**

in the TMA. **(E)** Representative IHC images showing the different levels and intensity of ER staining in the luminal B TMA cores. **(F)** Representative image of Krt5 IHC staining in luminal B TMAs. **(G)** p63 expression differences between luminal B and low-ER tumors. **(H-J)** Representative images of TSA staining showing homogeneous populations in luminal B TMAs and heterogeneous populations in low-ER TMAs. Samples were stained with Krt8 (purple), Krt5 (cyan), Krt14 (white), ER (green), and DAPI (blue). **(H)** Representative image of TSA staining showing homogeneous populations in luminal B TMAs. **(I)** Single channel images of luminal B TMA from Fig S2H. **(J)** Single channel images of low-ER TMAs from Fig 2H.

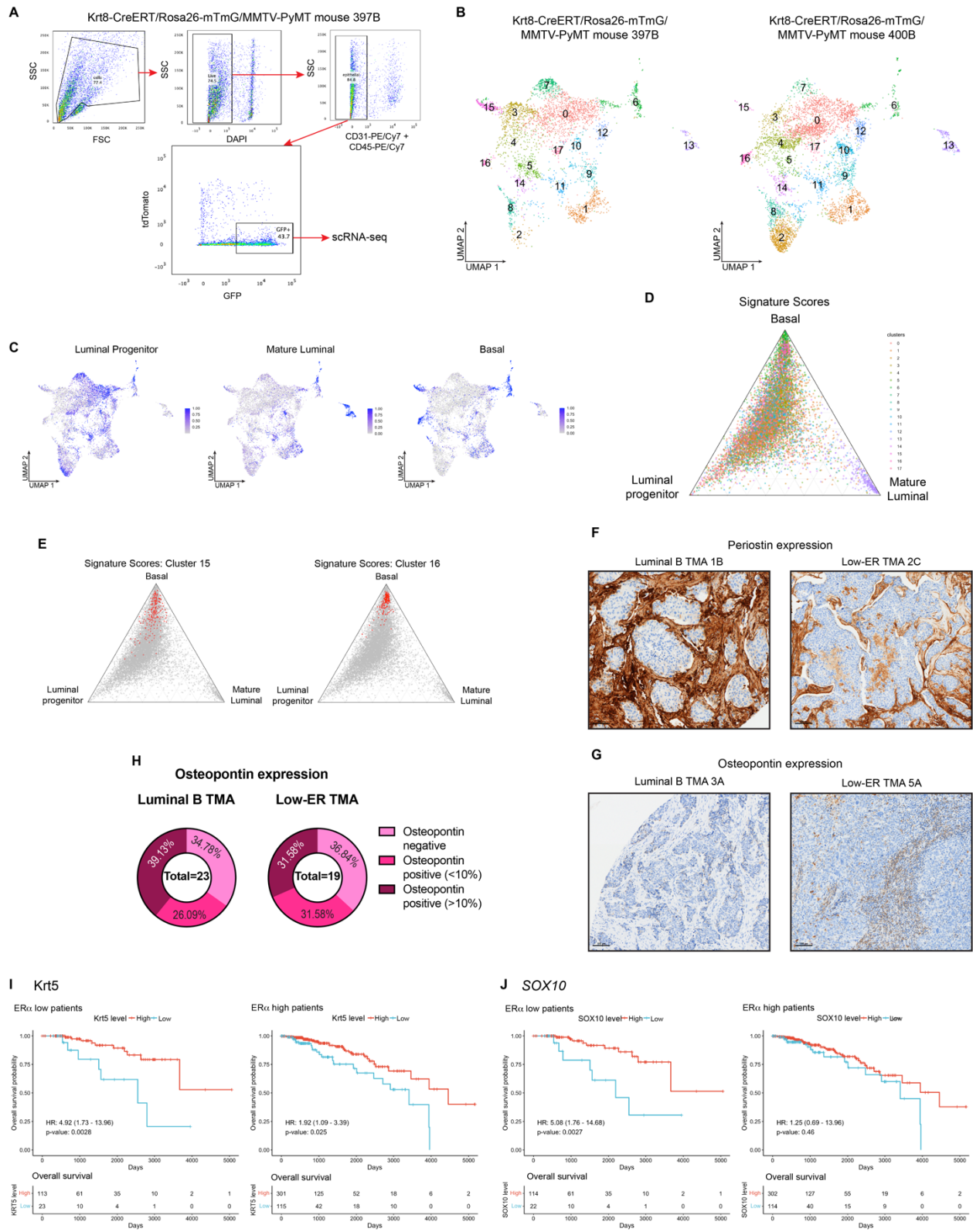


**Supplementary figure 3:** (A) Boxplots showing distribution of ER $\alpha$  levels in the ER+/PR- and ER+/PR+ cases used in this analysis. (B) Heatmap with unsupervised clustering of the basal signature gene expression in ER positive tumors. (C) Boxplots showing the differences in distribution of basal signature gene expression stratified by ER $\alpha$  expression level and PR status. (D) Boxplots showing distribution of *ESR1* levels in the ER+/PR- and ER+/PR+ cases used in this analysis. (E) Heatmap with unsupervised clustering of the basal signature gene expression in ER positive tumors. (F) Boxplots showing the differences in distribution of basal signature gene expression stratified by *ESR1* expression level and PR status. (G) Kaplan-Meier plot of overall survival in ER positive breast cancer cases from TCGA stratified by ER $\alpha$  expression.



**Supplementary figure 4: (A)** ER expression in MMTV-PyMT tumors. **(B)** Representative IHC images of ER expression in MMTV-PyMT tumors. **(C-D)** Optimization of tamoxifen induced GFP labelling in Krt5-CreERT/Rosa26-mTmG **(C)** and Krt8-CreERT/Rosa26-

mTmG **(D)** mouse mammary gland. **(E)** Flow cytometry gating strategy for identifying GFP expressing luminal and basal tumor cells. **(F-G)** Representative images of TSA staining of Krt5-CreERT/Rosa26-mTmG/MMTV-PyMT **(F)** and Krt8-CreERT/Rosa26-mTmG/MMTV-PyMT **(G)** tumors. Samples were stained with Krt8 (purple), Krt5 (red), Krt14 (white), and GFP (green). **(H)** Quantification of GFP expressing luminal and basal tumor cells from TSA stained images of Krt8-CreERT/Rosa26-mTmG/MMTV-PyMT tumors. **(I)** Single channel images of TSA staining of lung metastases from Krt8-CreERT/Rosa26-mTmG/MMTV-PyMT mice from Fig 4K showing no Krt14 expression. Samples were stained with Krt8 (purple), Krt14 (white), GFP (green), and DAPI (blue). **(J)** Counts of metastatic colonies from Krt5-CreERT/Rosa26-mTmG/MMTV-PyMT and Krt8-CreERT/Rosa26-mTmG/MMTV-PyMT mice expressing Krt8, Krt14, and GFP.





**Supplementary figure 5:** **(A)** Flow cytometry plots showing the gating strategy and the GFP positive cell population harvested using fluorescence assisted cells sorting (FACS). **(B)** UMAP of Krt8-CreERT/Rosa26-mTmG/MMTV-PyMT tumor cells sorted for GFP and split by sample of origin. Unsupervised clustering divided the cells into 18 different clusters. **(C)** Dimensionality reduction with UMAP of all tumor cells profiled with scRNA-seq. Cells are colored based on activity scores of luminal progenitor, mature luminal, and basal gene signatures. **(D)** Ternary plot showing the relative activity of luminal progenitor, mature luminal, and basal gene signatures across all tumor cells, colored by unsupervised cluster. **(E)** Ternary plots showing the distribution of relative activity of luminal progenitor, mature luminal, and basal gene signatures across all tumor cells profiled by scRNA-seq. In the left plot, cells assigned to cluster 15 are highlighted in red, while cells assigned to cluster 16 are highlighted in red in the right plot. **(F-G)** Representative images of periostin **(F)** and osteopontin **(G)** IHC staining in luminal B and low-ER TMAs. **(H)** Quantified osteopontin expression in luminal B and low-ER TMAs. **(I-J)** Kaplan-Meier plot of overall survival in ER positive breast cancer cases from TCGA stratified by Krt5 **(I)** and *SOX10* **(J)** expression in ER $\alpha$  low and ER $\alpha$  high cases.